Supporting Information for: Both genome and cytosol dynamics change in E.coli challenged with sub-lethal rifampicin

Michal Wlodarski, Bianca Raciti, Jurij Kotar, Marco Cosentino Lagomarsino, Gillian M. Fraser, and Pietro Cicuta*

Department of Physics, Cavendish Laboratory, University of Cambridge, JJ Thomson Avenue, Cambridge, CB3 0HE, United Kingdom

E-mail: pc245@cam.ac.uk

Phone: +44 (0)1223 746931. Fax: +44 (0)1223 337000

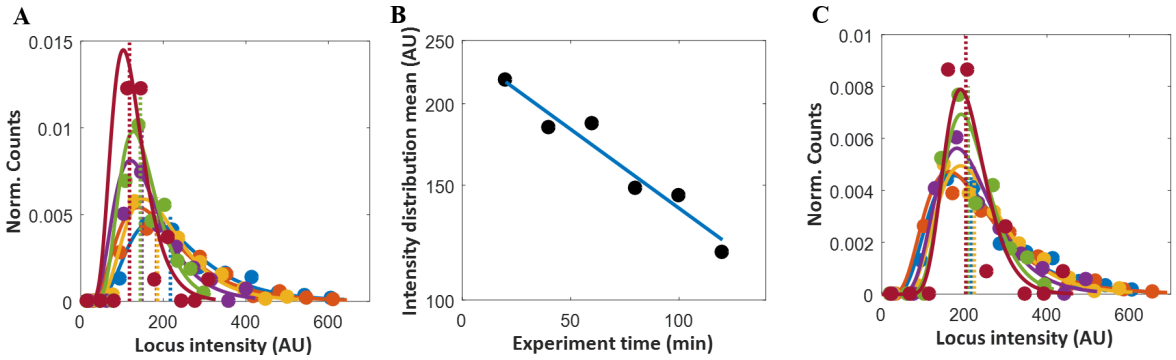

Figure S1. **Example data set of μNS-GFP cytosolic aggregates before and after photo-bleaching correction.** We calculate marker population bleaching rate and use it to calculate marker intensities. Plots show data for an example control (no drug) μNS-GFP sample. (**A**) Normalised log-normal marker intensity distributions for different experiment time points (20-120 min) (for function fitting details see Supplementary Materials). Part of the high end of the distribution tails is not shown. Dashed lines show means of the fitted distributions to demonstrate intensity-time dependence caused by photo-bleaching. (**B**) Distribution mean values from (**A**) over experiment time fitted with an exponential function (Equation S2, *blue line*). (**C**) Normalised log-normal marker intensity distributions for different experiment time points after calculating individual marker intensities.

Function fitting for data treatment

Marker intensity distribution and photo-bleaching profile fitting

To compare loci dynamics at various measurement times, effects of photo-bleaching must be accounted for first. We start by plotting frequency distributions of recorded loci intensities for individual measurement time points. We apply a cut-off to our intensity data at 100 AU as markers below this intensity value show significant static resolution errors, as shown previously. For this reason, we fit the data by generating maximum likelihood estimates of mean (μ) and standard deviation (σ) and then fit a log-normal probability density function, truncated at 100 AU, and then renormalized so that it integrates to one:

$$f(x) = \frac{\frac{1}{\sqrt{2\pi}\sigma x} e^{-(\log(x)-\mu)^2/2\sigma^2}}{1 - \frac{1}{\sigma\sqrt{2\pi}} \int_0^x \frac{e^{\frac{-(ln(t)-\mu)^2)}{2\sigma^2}}}{t} dt} \tag{S1}$$

The decay in distribution means (dashed vertical lines in Figure 2A and black solid circles

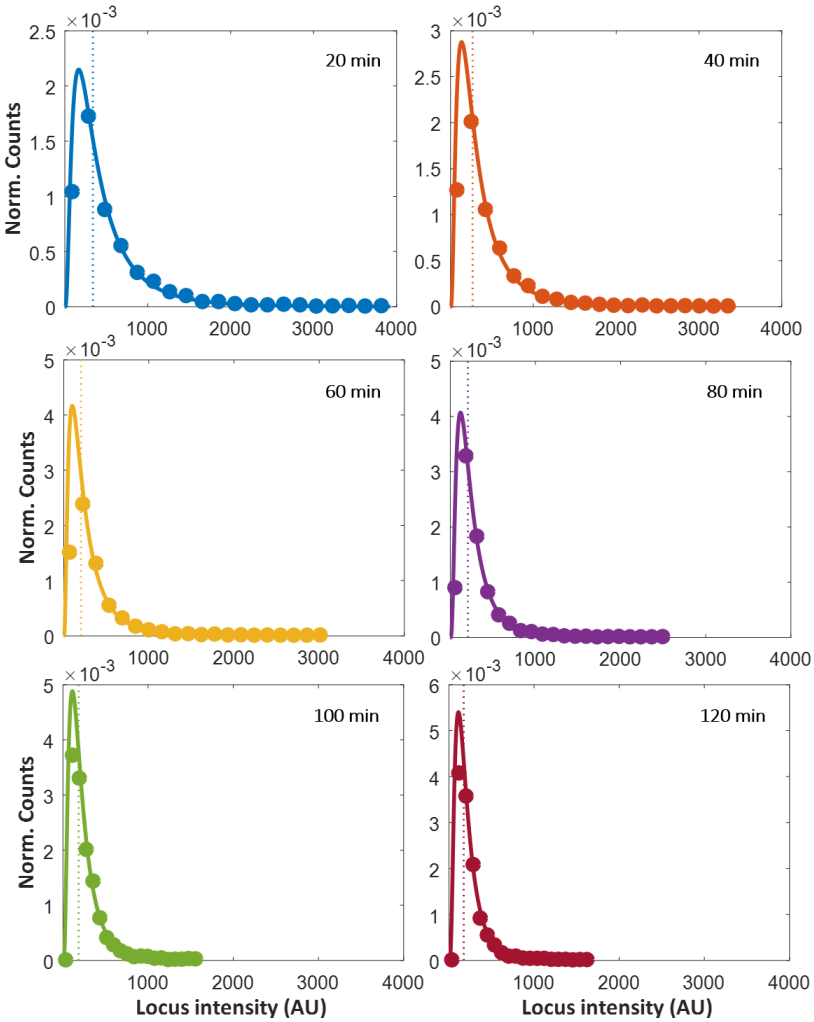

Figure S2. **Locus intensity distributions of an example Ori2 loci sample for individual measurement time points.** Distribution means are represented with dashed vertical lines.

in Figure 2B in main text) represents population photo-bleaching profile that can be fitted (Figure 2B) with an exponential function with a free baseline parameter for chromosomal loci (Equation 2, *main text*) or without a baseline parameter (for cytosolic aggregates to determine photo-bleaching rate):

$$I_t = I_0 e^{(-\lambda(t-t_0))}, \tag{S2}$$

where I_t is locus intensity at time t, I_0 is initial locus intensity at time t_0, t_0 is the initial measurement time (fixed at 20 min for all experiments), and λ is a free fitting parameter

representing the photo-bleaching rate. For each tracked locus, we use its population photo-bleaching rate, λ, to evaluate, using either Equation 2 (for chromosomal loci) or Equation S2 (for cytosolic aggregates), its original intensity (pre-photo-bleaching, I_0) assuming exponential decay in intensity.

Marker MSD–size dependence fitting

Once pre-photo-bleaching intensity of each locus at each measurement time point is determined, we proceed to correct for locus MSD–size dependence. Procedure is applied to MSDs at five arbitrary lag times (0.1, 1.0, 5.0, 10, and 14 s). For each lag time, we first arbitrarily segregate loci according their intensities by binning into 20 logarithmically-spaced bins along a 100-4,000 AU range and evaluate median MSD for each bin. We select medians for bins where the number of loci is equal of larger than the mean number of loci per bin (red solid circles in Figure 3A, *main text*) and fit those medians with a custom exponential function:

$$MSD_\tau(I) = p_1 e^{p_2 I}, \tag{S3}$$

where MSD_τ is MSD at one of the five lag times, τ, as a function of median binned locus intensity, I, and p_{1-2} are free fitting parameters.

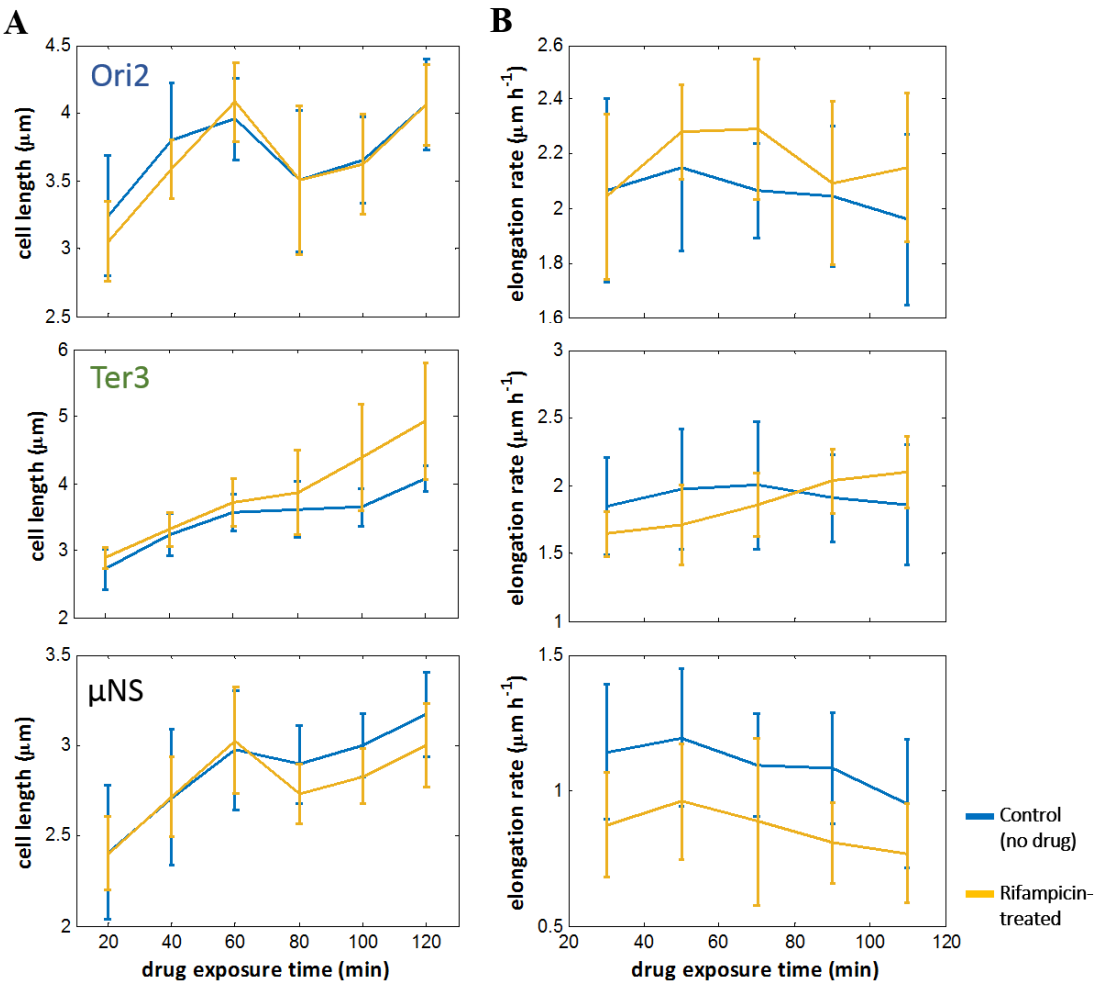

Figure S3. **Effects of rifampicin on cell lengths and elongation rates are small and not consistent between strains.** Figure shows cell length and elongation rate (as change in cell length in time) of the three *E. coli* strains (*top*, Ori2; *middle*, Ter3; *bottom*, μNS) used in this work over rifampicin treatment time (agarose data only). Controls (no drug) are in *blue* and effects of rifampcin are in *yellow*. Cell lengths were extracted from phase-contrast images for about 3,500 cells (443–691 per condition) until either cell division or end of experiment using a customised semi-automated MATLAB® program. **(A)** Cell length (μm) over drug exposure time (min). Cell lengths of control (no drug) cells generally increase over experiment time. Rifampcin effects are small, with Ter3 and μNS showing a small and consistent increase and decrease in cell length after ~60 min, respectively. **(B)** Cell elongation rate (μm h^{-1}) over drug exposure time (min). Elongation rates of control (no drug) cells are generally stable or slightly decrease over experiment time, with the exception of first two measurement times where there is a consistent increase possibly caused by bacteria adapting to new growth conditions. Rifampicin effects are small, with the μNS strain showing consistently lower rates throughout experiment.

Table S1. **Number of tracks and biological replicates for individual experiments.**

Agarose pad experiments								
		Ori2		Ter3		μNS		
experiment	biological replicates	control	rifamipcin	control	rifamipcin	control	rifamipcin	
1	3	7,985	1,986	1,456	4,718	1,230	784	
2	3	4,051	3,443	3,214	3,499	760	1,127	
3	3	1,728	2,528	1,694	2,649	-	-	
subtotals		13,764	7,957	6,364	10,866	1,990	1,911	
Microfluidic device experiments								
1	1	6,273	4,371	4,502	5,130	2,246	1,786	
totals		20,037	12,328	10,866	15,996	4,236	3,697	**67,160**